ELSEVIER

International Journal of Mass Spectrometry 202 (2000) 111–119

International Journal of Mass Spectrometry

Secondary cluster ion emission from megaelectron volts ion impacts on $NaBF_4$. 1. Ion decay fractions and dissociation pathways

M.J. Van Stipdonk[1], W.R. Ferrell,[2] D.R. Justes,[3] R.D. English, E.A. Schweikert*

Center for Chemical Characterization and Analysis, Department of Chemistry, Texas A&M University, P.O. Box 30012, College Station, TX 77842-3012, USA

Received 10 August 1999; accepted 6 March 2000

Abstract

Megaelectron volt ion impacts, event-by-event bombardment/detection, coincidence counting and a time-of-flight (TOF) mass spectrometer equipped with an electrostatic ion mirror were used to study the emission and dissociation of secondary cluster ions sputtered from sodium tetrafluoroborate ($NaBF_4$). The positive and negative plasma desorption spectra produced from $NaBF_4$ are distinct. The negative ion spectrum contains BF_4^- and cluster ions composed of Na^+ and BF_4^-, with a small series of peaks corresponding to $(NaF)_nF^-$. The positive spectrum, however, is dominated by a cluster ion series with composition $(NaF)_nNa^+$, $n = 0$–15. Magic numbers are observed in the positive cluster ion intensity distribution, highlighting $n = 4$ and 7 as stable cluster compositions. The presence of magic number enhancements in the linear TOF spectrum indicates that the stable cluster compositions are generated prior to entering the drift region of the TOF analyzer (i.e. during ion formation and acceleration). Decay fraction measurements demonstrate that both positive and negative secondary cluster ions carry residual internal energy and undergo dissociation reactions in the drift region of the TOF spectrometer. Decay pathway measurements show that the preferred neutral loss, in general, for positive and negative cluster ions is $(NaF)^0$. In the positive ion mode, the most probable dissociation pathway for many cluster ions is the formation of a product ion with a magic number composition. (Int J Mass Spectrom 202 (2000) 111–119) © 2000 Elsevier Science B.V.

Keywords: Cluster ions; Plasma desorption; Time-of-flight mass spectrometry; Metastable dissociation; Ion–Neutral correlations

1. Introduction

The impact of ^{252}Cf fission fragments (or similar energetic heavy ions) on certain organic and inorganic solids will produce positive ion mass spectra that are dominated by secondary ion peaks that resemble neither the composition nor structure of the original target material [1–4]. For instance, using plasma desorption mass spectrometry (PDMS) we have demonstrated that bombarding group IIA metal nitrate solids with ^{252}Cf fission fragments produce spectra

* Corresponding author: Texas A&M University, Center for Chemical Characterization & Analysis, Department of Chemistry, P.O. Box 30012, College Station, TX 77842-3012. E-mail: schweikert@mail.chem.tamu.edu

[1] Current address: Dr. Michael J. Van Stipdonk, Department of Chemistry, Wichita State University, Wichita, KS 67260-0051.

[2] Current address: Bayer Corporation, 8500 W. Bayer Road, Baytown, TX 77520-6451.

[3] Present address: Department of Chemistry, Penn State University, 152 Davey Lab, University Park, PA 16802.

PII S1387-3806(00)00238-4

primarily composed of secondary cluster ions with metal oxide compositions [5,6]. The negative ion spectra, however, feature secondary ion peaks characteristic of the metal nitrate composition.

Rabalais and co-workers examined the cluster ion emission from a series of complex inorganic salts using secondary ion mass spectrometry (SIMS) and keV atomic ion impacts (at low overall ion doses to minimize ion beam induced chemical damage) [7]. As a representative example, $NaBF_4$ contains the tetrahedral BF_4 anion in association with the metal cation. The analysis of a compound with three constituents, two of which share covalent bonds, allowed the composition of cluster ions to be compared to that of the original solid to probe for recombination or rearrangement reactions. The positive cluster ions sputtered from $NaBF_4$ by 5 keV energy Ar^+ ions were composed of only two of the sample's three constituent elements. No cluster ions containing all three constituents, nor BF_4^- intact, were observed. This result led to a conclusion that recombination or fast rearrangement was responsible for cluster ion formation from complex inorganic salts in SIMS.

Cluster ion formation from tetrafluoroborate salts has also been examined using PDMS [8,9]. The positive spectrum, as in the lower energy SIMS study, was dominated by a series of cluster ions following the composition trend $(NaF)_nNa^+$. In the PDMS experiments, negative ion mass spectra were also recorded. The most abundant peaks in the negative ion plasma desorption spectrum, however, were those corresponding to BF_4^- and cluster ions composed of Na^+ and BF_4^-. A less abundant cluster ion series with composition $(NaF)_nF^-$ was also observed. Subsequent studies of negative ion emission from $NaBF_4$ using kiloelectron volt energy atomic and polyatomic primary ions produced qualitatively similar results [10,11].

One of our research goals is to understand the chemical processes that underlie the formation of secondary ions following energetic ion impact. A clear understanding of the factors that determine secondary ion composition and abundance will facilitate the application of desorption/ionization mass spectrometry to surface characterization. The experiments described here build on our earlier qualitative study of the plasma desorption mass spectra generated from $NaBF_4$. In these experiments, megaelectron volt energy primary ions (^{252}Cf fission fragments), event-by-event bombardment/detection with coincidence counting and a time of flight (TOF) mass spectrometer equipped with an electrostatic ion mirror were used to study the emission of secondary cluster ions from $NaBF_4$. First, secondary ion decay fractions (the number of sputtered cluster ions that dissociate while in the first drift region of the mass spectrometer) were measured to probe residual secondary ion internal energy and ion stability. Second, using the ion–neutral correlation method, the pathways for positive and negative cluster ion dissociation reactions in the drift region of the mass analyzer were identified. This method was recently used to elucidate the dissociation pathways for metal oxide cluster ions sputtered from calcium, lanthanum and bismuth nitrate targets by megaelectron volt energy primary ions [12].

2. Experimental

2.1. Instrumentation

Mass spectra were collected using a TOF mass spectrometer recently constructed in our laboratory. The instrument configuration and operation have been described elsewhere [12]. Briefly, the instrument includes a vacuum chamber housing a ^{252}Cf radioactive source (megaelectron volt primary ion source), a sample target–acceleration grid assembly, a 25 mm diameter microchannel plate (MCP) start detector and a 40 mm diameter MCP reflected ion stop detector. An electrostatic ion mirror (or reflectron) is mounted to an extension connected to the vacuum chamber. An additional 40 mm MCP detector is located behind the ion mirror, and is used to collect linear TOF mass spectra or neutral spectra when voltage is applied to the mirror. Positive and negative plasma desorption mass spectra of $NaBF_4$ were acquired using an acceleration voltage of ± 8 kV. For reflected ion mass spectra and ion–neutral correlation metastable ion studies, a mirror voltage of ± 8835 V was used. This

value was obtained by adjusting the mirror voltage until the highest mass resolution for the sample specific peaks from *m/z* 65 to 191 was achieved (~2500 $M/\Delta M$).

2.2. Sample target preparation

Sample supports for these experiments consisted of aluminized Mylar™ stretched over and glued to stainless steel aperture plates. Solid $NaBF_4$ (Aldrich Chemical, St. Louis, MO) was dissolved in distilled/deionized water to a concentration of 0.3 M. A 10 μL aliquot of $NaBF_4$ solution was mixed with 10 μL of a dilute solution of methylcellulose in distilled water, transferred to the Mylar™ substrate and allowed to try under ambient conditions in a dark fume hood. The use of methylcellulose promotes wetting of the polymer support and induces thin, homogeneous surface coverage. The principal ion peaks observed from the methylcellulose additive are carbon and carbon/hydrogen cluster ions, which do not interfere with the detection and mass assignment of peaks representative of $NaBF_4$. Past studies have also shown that the presence of methylcellulose does not inhibit the generation or detection of sample specific secondary ions [10,13,14].

2.3. Decay fraction and ion dissociation pathway studies

A decay fraction is a relative measure of the number of secondary ions that dissociate to produce charged and neutral fragments in the drift region of the mass spectrometer. The decay fraction thus provides insight into relative ion internal energy and stability following sputtering and acceleration away from the sample surface. Decay fractions from $NaBF_4$ were measured by collecting two spectra each in the positive and negative ion modes. First, a mass spectrum was acquired with an acceleration voltage, $V_a = \pm 8.0$ kV and $V_{ref} = 0$. With these voltage settings, the linear TOF mass spectrum is a composite of stop events corresponding to intact ions and to ion and neutral fragments from in-flight dissociation. Next, a spectrum was acquired with $V_a = \pm 8.0$ kV and $V_{ref} = 10.0$ kV, the latter voltage set to reject all ionized species. The linear TOF spectrum in this case provides a measure of the stop events corresponding to neutral species created by in-flight dissociation reactions. The decay fraction is then calculated using the formula

$$\text{decay fraction} = I_{\text{neutrals}}/I_{\text{ions+neutrals}}$$

where I_{neutrals} corresponds to the peak area of a particular peak with V_r set to reject all ionized species (i.e. higher than V_a) and $I_{\text{ions+neutrals}}$ is the peak area of the same peak measured with the V_r set to 0 V. Because the same MCP detector is used for both measurements, the detection efficiencies (which depend on particle velocity) for the $I_{\text{ions+neutrals}}$ and I_{neutrals} measurements are effectively the same. We assume that the net collection efficiency for the intact and fragment species for each cluster parent ion is the same. The angular distributions for neutral and ion fragments that arise from dissociation reaction within the drift region of this TOF instrument are not known.

The methodology for studying ion–neutral correlations from the metastable dissociation of secondary ions in a reflecting TOF instrument was developed by Della Negra and co-workers [15,16] and has been used to study the dissociation of a wide range of secondary ions [17–21]. We have adapted the method to include our coincidence-counting data acquisition software: a description of the protocol used in our laboratory was described in detail recently [22].

The ion and neutral fragments generated from discrete ion dissociation events can be separated using the electric field within an electrostatic mirror. The field will reflect secondary ions that remain intact, along with fragment ions from dissociation reactions. The neutral species from in-flight dissociation are not affected by the electric field and pass through the mirror to strike the direct detector. Due to conservation of momentum, the neutral from a particular precursor ion will have a linear flight time nearly equal to the precursor ion, and the neutral can be used to identify the dissociating ion.

To correlate the neutral and ion fragments that originate from the same dissociating ion, coincidence

windows were set to include the width (typically 50–100 ns wide) of a particular neutral peak attributed to in-flight dissociation (as opposed to neutrals formed within the acceleration region, which are shifted to higher flight time according to changes in acceleration energy) as detected using the MCP detector behind the electrostatic mirror. The neutral peaks were separated by at least 1 μs, allowing neutrals from each dissociation precursor ion to be completely resolved in time. The coincidence software then registers correlated ion stop events at the reflected ion MCP detector within the entire 64 μs TDC acquisition time following a trigger by a fission fragment start signal. Using a coincidence window, a coincidence spectrum is obtained which contains all of the stop events registered at the reflected detector in coincidence with the start signal/fission fragment impact and the detection of a particular neutral species. The current software design allows up to ten dissociation pathways to be monitored simultaneously.

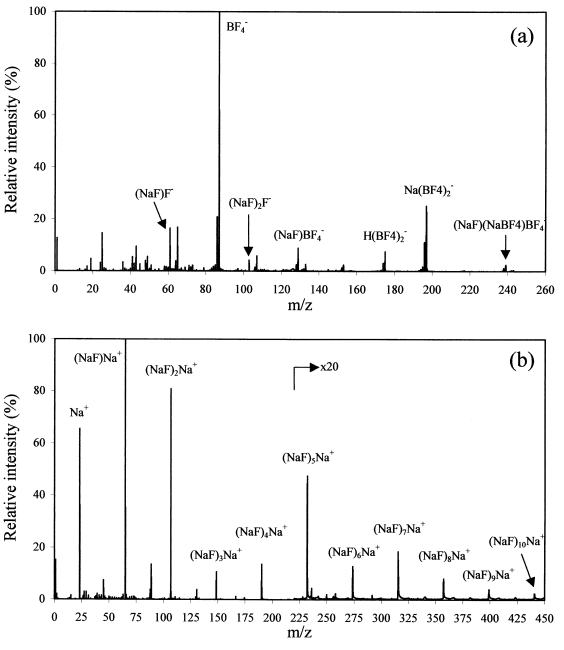

Fig. 1. Negative (a) and positive (b) secondary ion mass spectra produced by ^{252}Cf fission fragment impacts on $NaBF_4$. Both spectra were collected in the linear TOF mode.

3. Results and discussion

3.1. Negative and positive ion mass spectra

Figure 1 shows the (a) negative and (b) positive ion spectra produced from $NaBF_4$ by ^{252}Cf fission fragments. Both spectra were collected in the linear mode (i.e. the voltage on the electrostatic mirror was set at 0 V). Qualitatively similar negative and positive ion mass spectra were obtained in the reflected ion mode.

The major sample relevant secondary ions observed and their measured mass to charge ratios are provided in Table 1. As observed in earlier work [8], the fission fragment projectiles produce distinct negative and positive ion mass spectra. The majority of the negative ion species observed from fission fragment impacts are composed of Na^+ and BF_4^-. In addition, minor peaks were observed that contain (NaF) units, including a cluster series with composition $(NaF)_nF^-$ (n = 1–3). Using kiloelectron volt energy atomic and polyatomic primary ions and TOF mass spectrometry, we have demonstrated that the negative SIMS spectra of $NaBF_4$ are predominantly composed of ions such as BF_4^- and $(NaBF_4)BF_4^-$ [10,11]. Thus the negative spectra produced by PDMS and SIMS contain secondary ion signals that accurately reflect the composition and stoichiometry of the $NaBF_4$ solid.

The positive PDMS spectrum, however, is dominated by a series of cluster ions with composition $(NaF)_nNa^+$ (n = 1–15). A less abundant cluster series following the composition trend $(NaBF_4)_nNa^+$ (n = 1–3) was also observed. The former series was also reported for 5 keV Ar^+ impacts on $NaBF_4$ [7]. In the SIMS experiments, however, a series of cluster ions composed of Na^+ and BF_4^- was not observed.

The positive cluster ions provide clear evidence for the generation of recombination and/or rearrangement reactions during ion formation following ^{252}Cf fission fragment impact. Because of the omission of B, the positive secondary cluster ions sputtered from $NaBF_4$ resemble those expected from the sputtering of a sodium fluoride (NaF) target. The $(NaF)_nNa^+$ cluster

Table 1
Positive and negative secondary ions observed following ^{252}Cf fission fragment impacts on $NaBF_4$; for secondary species that include a boron atom, only the *m/z* value of the ion containing the ^{11}B isotope is shown

	m/z
Negative ion composition	
F^-	19
$(NaF)F^-$	61
BF_4^-	87
$(NaF)_2F^-$	103
$(NaF)BF_4^-$	129
$(HBF_4)BF_4^-$	175
$(NaBF_4)BF_4^-$	197
$(NaBF_4)(NaF)BF_4^-$	239
Positive ion composition	
Na^+	23
$(NaF)Na^+$	65
$(HBF_4)H^+$	89
$(NaF)_2Na^+$	107
$(NaBF_4)Na^+$	133
$(NaF)_3Na^+$	149
$(NaF)(NaBF_4)Na^+$	175
$(NaF)_4Na^+$	191
$(NaF)_5Na^+$	233
$(NaF)_6Na^+$	275
$(NaF)_7Na^+$	317
$(NaF)_8Na^+$	359
$(NaF)_9Na^+$	401
$(NaF)_{10}Na^+$	443
$(NaF)_{11}Na^+$	485
$(NaF)_{12}Na^+$	527
$(NaF)_{13}Na^+$	569
$(NaF)_{14}Na^+$	611
$(NaF)_{15}Na^+$	653

ion intensity distribution, in general, decreases with increasing mass. The intensity distribution is not smooth, however, and the formation of cluster ions with $n = 4$ and 7 is favored over cluster ions with $n = 3$ and 6. The appearance of these well-known "magic numbers" demonstrates the enhanced stability in the gas phase of cluster ions with certain numbers of constituents [23]. Theoretical studies of alkali halide clusters have shown that the magic numbers represent stable, cubic shaped representatives of the solid-state crystal structure [24]. For instance, the lowest energy configurations predicted for cluster species at $n = 4$ and $n = 7$ are $3 \times 3 \times 1$ and $3 \times 5 \times 1$ lattice structures, respectively.

The observation of magic numbers at $n = 4$ and 7 in the $(NaF)_nNa^+$ cluster intensity distribution from $NaBF_4$ is consistent with an earlier study of the sputtering of alkali halides by kiloelectron volt atomic ion impacts [23,25]. One major difference between the present work and earlier SIMS studies is the potential to use a TOF analyzer to determine the influence of metastable dissociation on the cluster ion intensity distribution. In SIMS instruments that employ magnetic sector or quadrupole mass analyzers, sputtered cluster ions must survive the transit time through the mass analyzer (i.e. hundreds of microseconds) to be detected at their original intact mass. Metastable dissociation reactions that occur on μsec time scales will alter the secondary ion intensity distribution (those ions that dissociate will not be detected at their original mass), and thus will enhance the abundance of cluster ions with magic number compositions. Using a TOF-SIMS instrument, which requires only that an ion survive the acceleration step (tens of nanoseconds) to be detected at its original mass, Ens et al. demonstrated that $(CsI)_nCs^+$ cluster ions sputtered from a cesium iodide target produce a smooth, near exponential decay intensity distribution [26]. Since a linear TOF instrument probes the ion intensity distribution prior to any alteration due to metastable or unimolecular decomposition reactions (with the caveat that decomposition in the acceleration will affect the intensity distribution), the conclusion made in reference [26] was that the anomalies in the $(CsI)_nCs^+$ intensity distribution were not due to ion production processes. In the present study, the secondary cluster ions generated by megaelectron volt ion impacts were also mass analyzed by TOF in the linear and reflected ion mode. The fact that they appear in our linear TOF spectrum indicates that the magic numbers in the distribution $(NaF)_nNa$ cluster ions sputtered from $NaBF_4$ are generated before entering the drift region, presumably during ion formation and acceleration away from the surface. Because these experiments were carried out using event-by-event bombardment, recombination from multiple ion impacts and/or chemical damage effects due to a high overall ion

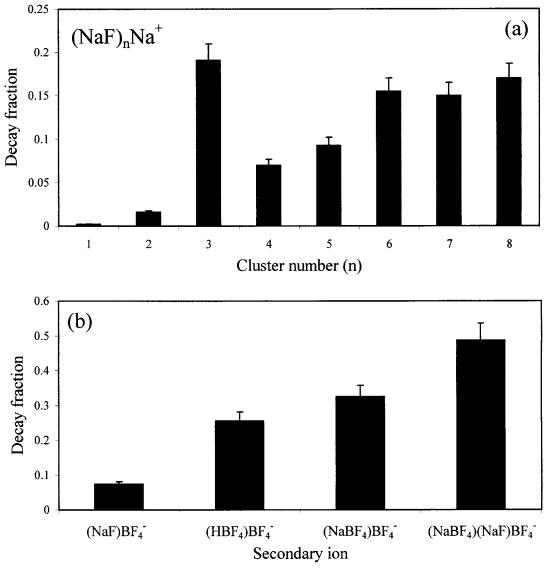

Fig. 2. Decay fraction measurements for (a) negative and (b) positive secondary cluster ions emitted from $NaBF_4$ following ^{252}Cf fission fragment impacts. Decay fractions were calculated as described in Sec. 2.

dose can be ruled out as a cause for the observed trends.

3.2. Decay fraction measurements

Fig. 2 shows the decay fraction measurements for positive [Fig. 2(a)] and negative [Fig. 2(b)] secondary cluster ions sputtered from $NaBF_4$ by ^{252}Cf fission fragments. In general, the decay fractions for the $(NaF)_nNa$ cluster species observed in the positive PDMS spectrum increase with the size of the ion. An increase in decay fraction with increasing cluster ion size was also observed for $(Bi_2O_3)_nBiO^+$ clusters sputtered by megaelectron volt ion impacts on $Bi(NO_3)_3$ [12], and for ammonia cluster ions by Castleman and co-workers [27]. The trend can be explained by a general decrease in binding energy with increasing cluster ion size.

As with the ion intensity distribution, however, the decay fraction increase for the $(NaF)_nNa^+$ cluster ions is not smooth. The decay fraction for the $n = 3$ cluster ion is considerably higher than the decay fraction exhibited by the $n = 2$ and $n = 4$ species, indicating that the seven atom cluster ion is particularly unstable. In addition, the cluster at $n = 6$ is less stable than the cluster ions at $n = 5$ and $n = 7$. We recently showed that intensity anomalies also appear in the decay fraction distribution for $(CaO)_nH^+$ cluster ions sputtered from $Ca(NO_3)_2$ by ^{252}Cf fission fragment impacts. The high decay fractions at $n = 3$ and 6 demonstrate the instability of cluster ions immediately preceding a cluster ion with magic number composition, i.e. $n = 4$ and 7, due perhaps to a lower activation energy for the dissociation reaction for cluster ions with these particular compositions and configurations. The instability of alkali halide cluster ions to metastable dissociation has also been rationalized based on a consideration of cluster surface energy [28]. High surface energy regions due to incomplete cubic faces (in the case where the cluster ions adopt cubic packed structures) will presumably lead to greater instability.

The decay fractions for the negative cluster species also increase with increasing secondary ion mass. Of particular interest are the higher overall decay fraction values compared to the positive cluster ions. This indicates that the negative cluster ions are less stable, in general, than the positive cluster ions. One plausible route to the production of a neutral species from a negative cluster ion is electron detachment. The decay fraction measurements do not determine the percentage of the neutral species formation due to electron detachment relative to the percentage attributable to a cluster dissociation reaction. Our results indicate, however, that up to 50% of some negative cluster ions sputtered from the surface will decay or neutralize within the TOF drift region of a reflectron based mass spectrometer with a design similar to the one employed for these experiments. The decay fraction measured will depend, in part on the length of the flight region and the acceleration voltage used (both of which determine the time an ion spends in the drift region of the instrument). The time window for cluster ion dissociation within the TOF drift region used for these experiments was approximately $10^{-8} \Rightarrow 10^{-5}$ s following the fission fragment impact. The decay fractions measured for the negative cluster ions may be of concern in situations where reflecting TOF

Table 2
Negative cluster ion dissociation pathways determined using the ion–neutral correlation method

$BF_4^- \Rightarrow BF_3^0 + F^-$
$(NaF)BF_4^- \Rightarrow (NaF)^0 + BF_4^-$
$(HBF_4)BF_4^- \Rightarrow (HBF_4)^0 + BF_4^-$
$(NaBF_4)BF_4^- \Rightarrow (NaBF_4)^0 + BF_4^-$
$Na(BF_4)_2(NaF)^- \Rightarrow (NaF)^0 + (NaBF_4)BF_4^-$

instruments are employed to obtain high resolution mass spectra of inorganic polyatomic anions. An increase in decay fraction leads to a proportional decrease in reflected ion signal.

3.3. Dissociation pathways

Using coincidence counting and the ion–neutral correlation method [12,15], the pathways for dissociation reactions occurring in the first drift region of the TOF analyzer were determined. The dissociation pathways for the negative cluster ions sputtered from $NaBF_4$ by ^{252}Cf fission fragments are shown in Table 2. The dissociation of the BF_4 ion leads to F^- as the product ion with a stable BF_3 molecule likely shed as the neutral species. The $(HBF_4)BF_4$ and $(NaBF_4)BF_4$ cluster ions each dissociate to produce a BF_4^- product ion. The $(NaF)BF_4^-$ and $\{Na(BF_4)_2(NaF)\}^-$ ions, mixed anion species composed of Na^+, F^-, and BF_4^-, generate BF_4^- and $(NaBF_4)BF_4^-$ product ions, respectively, in both cases the neutral loss corresponds to a (NaF) unit.

The pathways discerned for the in-flight dissociation reactions for the $(NaF)_nNa^+$ cluster ions are listed in Table 3. The general dissociation pathway for each cluster ion involves the evaporation of one or more neutral (NaF) units. Based on a comparison of SIMS data of the stability of NaCl cluster ions sputtered by kiloelectron volt energy Xe ions to theoretical predictions by Martin [24], Barlak et al. postulated that the most favorable dissociation pathway for $(NaCl)_nNa^+$ ions is the emission of neutral (NaCl) units [25]. The present study demonstrates that the same is true for the dissociation of $(NaF)_nNa^+$ cluster ions sputtered from $NaBF_4$.

The cluster ions with $n = 4$, 5, 7, and 8 show

Table 3
Positive cluster ion dissociation pathways determined using the ion–neutral correlation method

$(NaF)_2Na^+ \Rightarrow (NaF)^0 + (NaF)Na^+$
$(NaF)_3Na^+ \Rightarrow (NaF)_2^0 + (NaF)Na^+$
$(NaF)_4Na^+ \Rightarrow (NaF)_3^0 + (NaF)Na^+$ (73%)
$\Rightarrow (NaF)_2^0 + (NaF)_2Na^+$ (27%)
$(NaF)_5Na^+ \Rightarrow (NaF)_2^0 + (NaF)_3Na^+$ (14%)
$\Rightarrow (NaF)^0 + (NaF)_4Na^+$ (86%)
$(NaF)_6Na^+ \Rightarrow (NaF)_2^0 + (NaF)_4Na^+$
$(NaF)_7Na^+ \Rightarrow (NaF)_3^0 + (NaF)_4Na^+$ (83%)
$\Rightarrow (NaF)_2^0 + (NaF)_5Na^+$ (17%)
$(NaF)_8Na^+ \Rightarrow (NaF)^0 + (NaF)_7Na^+$ (14%)
$\Rightarrow (NaF)_2^0 + (NaF)_5Na^+$ (26%)
$\Rightarrow (NaF)_4^0 + (NaF)_4Na^+$ (60%)
$(NaF)_9Na^+ \Rightarrow (NaF)_2^0 + (NaF)_7Na^+$
$(NaF)_{10}Na^+ \Rightarrow (NaF)_2^0 + (NaF)_8Na^+$

multiple dissociation pathways. Of note is the fact that the most probable dissociation pathway for many of the positive cluster ions leads to the formation of product ions with magic number compositions. For instance, the $n = 5$, 6, 7, and 8 cluster ions all show a dissociation pathway that leads to the formation of an $n = 4$ product ion. The $n = 8$ and 9 cluster ions both show dissociation pathways that lead to an $n = 7$ product ion. Combining the probability for dissociation by the $n = 8$ cluster ion into $n = 4$ and $n = 7$ product ions, the $n = 4$, 5, 7, and 8 cluster ions, where multiple channels exist, dissociate to a magic number composition better than 70% of the time. Despite the fact that the $n = 1$ cluster ion is also stable, only the $n = 2$, 3, and 4 cluster ions exhibit a dissociation channel to an $n = 1$ product ion. Thus the dissociation pathways of the larger cluster ions are influenced to a large extent by the stability of the $n = 4$ and $n = 7$ product ions.

4. Conclusions

In these experiments, event-by-event bombardment and detection, coincidence counting and a reflecting TOF mass spectrometer were used to measure the decay fractions and dissociation pathways for positive and negative secondary ions sputtered from $NaBF_4$ by ^{252}Cf fission fragments. In accord with an earlier preliminary study, the negative and positive

ion mass spectra produced from $NaBF_4$ are distinct in terms of their analytical utility. The negative ion spectrum contains abundant ion signal that relates directly back to the composition of the sample material. The positive spectrum, however, in dominated by a $(NaF)_nNa^+$ cluster ion series, complete with intensity enhancements at the magic number values of $n = 4$ and 7. The similarity between the PDMS results, using ~100 MeV ion impacts, and those obtained using kiloelectron volt energy atomic primary ions [7,23,25] indicate that high-energy projectile impacts are not necessary to generate the cluster ion intensity distributions observed. The qualitative features of the positive ion mass spectrum are therefore tied to ion formation processes determined by the starting material, $NaBF_4$, and are independent of primary projectile characteristics.

The positive secondary cluster ion emission from solid $NaBF_4$ is particularly interesting. It is clear that ion impacts, whether at megaelectron volt or kiloelectron volt energies, induce disproportionation reactions to produce secondary product ions that are composed predominantly of Na and F. The magic numbers that were observed in both the linear and reflected positive ion mass spectra are indicative of the adoption of stable, rock-salt type structures. Their presence in the linear mode TOF spectrum indicates that, to a large extent, the magic number anomalies in the positive cluster ion distribution arise shortly after primary ion impact, either during ion formation or acceleration from the surface but before entering the drift region. The cluster ion distribution continues to be modified by dissociation reactions in the drift region of the TOF spectrometer.

Pronounced tails to the high flight time side of the peaks at $n = 4$ and $n = 7$ are observed in the reflected ion mass spectrum. The tails provide evidence that a portion of the $n = 4$ and 7 cluster ions are formed by the dissociation of larger secondary ions within the acceleration region of the instrument. Based on the dimensions and voltage settings of the secondary ion source region of our instrument, the time window for these dissociation reactions is from $\sim 10^{-11}$ to 10^{-8} seconds following ion impact. Work on a thorough analysis of the peak tails, along with measurements of the initial kinetic energy distributions of the positive and negative cluster ions from $NaBF_4$ is in progress and will be the subject of a future publication.

The decay fraction measurements for the $(NaF)_nNa^+$ cluster ions demonstrate that the cluster ion intensity distribution continues to evolve via metastable dissociation reactions in the TOF drift region. The decay fractions indicate that certain cluster ions, such as those at $n = 3$ and 6 are particularly unstable. While an increase in decay fraction is observed for $n = 1$–6, beyond $n = 7$ the cluster ion decay fractions are constant. The decay fraction measurements show that the negative ions, in general, are less stable than the positive secondary ions.

Using coincidence counting and the ion-neutral correlation method, the dissociation pathways for several negative and positive cluster ions were determined. Our results contribute to previous applications of this method to produce "tandem-mass spectrometry" type information from a reflecting TOF mass spectrometer [17–21]. The dissociation of the negative cluster ions featured the loss of (NaF) units to form BF_4^- and $(NaBF_4)BF_4^-$ product ions. The same neutral loss was predominant in the positive ion mode. Each $(NaF)_nNa^+$ cluster ion dissociated by shedding one or more (NaF) unit, and for cluster ions larger than $n = 4$, the main dissociation pathways lead to the formation of product ions with $n = 4$ and $n = 7$ compositions.

Acknowledgements

The authors would like to thank J.F. Blankenship and E.F. da Silviera for important early contributions to this work. Support from the National Science Foundation (grant no. CHE-9727474) is also acknowledged.

References

[1] M.J. Van Stipdonk, E.A. Schweikert, Nucl. Instrum. Methods Phys. Res. B 96 (1995) 530.
[2] L. Schmidt, H. Jungclas, Proceedings of the Third Interna-

tional Congress on Ion Formation from Organic Solids (IFOS IV), 1987, p. 91.
[3] P. Weiland, K. Wien, S. Della-Negra, J. Depauw, J. Joret, Y. Le Beyec, J. Phys. 50 (1989) 141.
[4] G. Brinkmalm, D. Barofsky, P. Demirev, D. Feynö, P. Håkansson, R.E. Johnson, C.T. Reimann, B.U.R. Sundqvist, Chem. Phys. Lett. 191 (1992) 345.
[5] W.R. Ferrell, M.J. Van Stipdonk, E.A. Schweikert, Nucl. Instrum. Methods Phys. Res. B 112 (1996) 55.
[6] W.R. Ferrell, S.L. von Heimburg, M.J. Van Stipdonk, E.A. Schweikert, Int. J. Mass Spectrom. Ion Processes 155 (1996) 89.
[7] F. Honda, G.M. Lancaster, Y. Fukuda, J.W. Rabalais, J. Chem. Phys. 69 (1978) 4931.
[8] M.J. Van Stipdonk, Ph.D. dissertation, Texas A&M University, 1994.
[9] M.J. Van Stipdonk, J.B. Shapiro, E.A. Schweikert, Vacuum 46 (1995) 1227.
[10] M.J. Van Stipdonk, R.D. Harris, E.A. Schweikert, Rapid Commun. Mass Spectrom. 11 (1997) 1794.
[11] M.J. Van Stipdonk, V. Santiago, E.A. Schweikert, J. Mass Spectrom. 34 (1999) 554.
[12] M.J. Van Stipdonk, D.R. Justes, R.D. English, E.A. Schweikert, J. Mass Spectrom. 34 (1999) 677.
[13] J.F. Blankenship, M.J. Van Stipdonk, E.A. Schweikert, Rapid Commun. Mass Spectrom. 11 (1997) 143.
[14] M.J. Van Stipdonk, D.R. Justes, V. Santiago, E.A. Schweikert, Rapid Commun. Mass Spectrom. 12 (1998) 1639.
[15] S. Della Negra, Y. LeBeyec, Anal. Chem. 57 (1985) 2036.
[16] A. Brunelle, S. Della Negra, J. Depauw, H. Joret, Y. Le Beyec, in Ion Formation from Organic Solids (IFOS V), A. Hedin, B.U.R. Sundqvist, A. Benninghoven (Eds.), Wiley, Chinchester, 1990 p. 39.
[17] S. Bouchonnet, J-P. Denhez, Y. Hoppilliard, C. Mauriac, Anal. Chem. 64 (1992) 742.
[18] X. Tang, R. Beavis, W. Ens, S. LaFortune, B. Schueler, K.G. Standing, Int. J. Mass Spectrom. Ion Processes 85 (1988) 43.
[19] X. Tang, W. Ens, K.G. Standing, J.B. Westmore, Anal. Chem. 60 (1988) 1791.
[20] A. Brunelle, S. Della Negra, J. Depauw, H. Joret, Y. LeBeyec, Rapid Commun. Mass Spectrom. 5 (1991) 40.
[21] M.J. Van Stipdonk, E.A. Schweikert, Nucl. Instrum. Methods Phys. Res. B 112 (1996) 68.
[22] M.J. Van Stipdonk, E.A. Schweikert, M.A. Park, J. Mass Spectrom. 32 (1997) 1151.
[23] J.A. Taylor, J.W. Rabalais, Surf. Sci. 74 (1978) 229.
[24] T.P. Martin, J. Chem. Phys. 72 (1980) 3506.
[25] T.M. Barlak, J.E. Campana, J.R. Wyatt, R.J. Colton, J. Phys. Chem. 87 (1983) 3441.
[26] W. Ens, R. Beavis, K.G. Standing, Phys. Rev. Lett. 50 (1983) 27.
[27] S. Wei, A.W. Castleman Jr., Int. J. Mass Spectrom. Ion Processes 131 (1994) 233.
[28] J.E. Campana, B.N. Green, J. Am. Chem. Soc. 106 (1984) 531.